ICANS-VI

INTERNATIONAL COLLABORATION ON ADVANCED NEUTRON SOURCES

June 27 - July 2, 1982

# STATUS OF THE WNR/PSR AT LOS ALAMOS

R. N. Silver
Physics Division
Los Alamos National Laboratory
Los Alamos, NM 87545

## ABSTRACT

A proton storage ring is presently under construction at Los Alamos for initial operation in 1985 to provide the world's highest peak neutron flux for neutron scattering experiments. The operational WNR pulsed neutron source is in use for TOF instrument development and condensed matter research. Experimental results have been obtained in incoherent inelastic scattering, liquids and powder diffraction, single crystal diffraction and eV spectroscopy using nuclear resonances. Technical problems being addressed include chopper phasing, scintillator detector development, shielding and collimation. A crystal analyzer spectrometer in the "constant Q" configuration is being assembled. The long range plan for the WNR/PSR facility is described.

The Los Alamos pulsed spallation neutron source, the WNR/PSR is progressing toward its goal of a world class facility in 1985. This will provide a peak thermal flux of $10^{16}$ n/cm$^2$-s at 12Hz, with a time average current of 100 μA of 800 MeV protons. Construction has commenced on the Proton Storage Ring (PSR), which will compress the 750 μ sec long macropulses from the LAMPF accelerator to a .27 μsec proton pulse width more suitable for time of flight neutron scattering experiments. Construction is presently on schedule and within cost, with the first proton beam expected in March 1985.

In this paper, the emphasis will be on the progress and plans of the neutron scattering research program and instrumentation at Los Alamos. The WNR is presently an operational spallation neutron source, with a time average current of 4-5 μA of 800 MeV protons at a proton pulse width of 5 μsec and a repetition rate of 120Hz. This makes it possible to test novel TOF instrument developments, to explore the unique science made possible by these sources, and to develop the expertise of the scientific staff by research experience. The goal is to have mature instrumentation, research programs, and staff by 1986 to maximize the scientific impact of the much superior source characteristics of the PSR.

Neutron scattering instrumentation at Los Alamos has advanced considerably since the last report at ICANS IV. Figure 1 shows the current layout of instrumentation at the WNR. Three instruments, which were in an assembly or testing stage two years ago, are presently in a production mode for condensed matter research. These are: 1) a general purpose diffractometer (GPD) for powder,

liquids, and amorphous materials diffraction; 2) a single crystal diffractometer (SCD) based on the Laue-TOF technique; and 3) a Be-BeO filter difference spectrometer (FDS) for incoherent inelastic scattering. A prototype eV spectrometer using nuclear resonance filters (EVS) is operational. Testing and assembly has commenced on a constant Q spectrometer for the measurement of elementary excitations in single crystals, particularly at high energies. In addition, the vexing problem of phasing neutron choppers to the power line used to trigger LAMPF has been solved. Systematic studies have commenced of shielding and data acquisition requirements for the much higher intensities of the PSR era.

The filter difference spectrometer, shown in Figure 2, uses the differing Bragg cutoffs of Be and BeO to improve the resolution of the filter detector techniques (see the article by J. A. Goldstone, et.al., in these proceedings). Figure 3a shows the raw Be filter spectrum from KH Maleate, while Figure 3b shows the improvement in resolution obtained by taking the difference of Be and BeO filter spectra. A comparison of the performance of the FDS with the crystal analyzer spectrometer (CAS) (Figure 4) is shown in Figure 5. These were obtained on approximately 30g samples with 100 μA-hrs of beam. The FDS has comparable resolution to the CAS with greatly improved count rate. In the final version, a further factor of 4 improvement will be obtained for the FDS by cooling the filters to 77°K and increasing the detector solid angle. An example of research with the FDS is shown in Figure 6 and 7. Ni-Dimethylgloxine is a molecule with an intramolecular hydrogen

bond. The vibrational frequency of the out of plane bending mode $\gamma$(OHO) of this hydrogen is obtained by observing the change in spectrum upon deuteration (Figure 6). Measurements of this kind were used in a systematic study of the variation of the vibrational frequency with bond length. The question was whether the trend observed with the longer bonds of the intermolecular cases would continue for the shorter bonds of the intramolecular cases. The results (Figure 7) show a clearly different trend. The FDS and CAS have also been used for studies of hydrogen optic modes in metal hydrides and for complementary measurements to IR and Raman in chemical spectroscopy.

The general purpose diffractometer is shown in Figure 7. The 150° bank provides for medium resolution ($\Delta d/d \sim .45\%$) powder diffraction. The low angle banks at 40° and 10° are especially important to minimizing inelasticity connections in liquids diffraction. In this paper, the emphasis will be on recent work on the structure of water with the GPD. The quantity sought in a diffraction experiment is the static structure factor S(Q). However, the quantity measured is a differential cross section $\Sigma$(Q). These are simply related to each other only in the case of completely elastic scattering. In the case of light elements, the recoil of the particle from which the neutron scatters leads to large inelasticity corrections required to extract S(Q) from $\Sigma$(Q). Examination of the kinematics shows that the corrections can be minimized by scattering at low angles with high energy neutrons to achieve a given Q. This is demonstrated in a comparison of the

performance of the GPD with the D4 instrument at the ILL shown in Figure 8. The structure factor S(Q) is expected to oscillate about the static self scattering limit at high Q. However, the measured cross section at the ILL droops far below the self scattering limit. At a reactor, high Q is reached at a fixed wavelength by scattering at large angles with a consequent large inelasticity correction. In contrast, the result for the GPD at 40° is much closer to the static limit because high energy neutrons (up to 1.7 eV at $20\text{Å}^{-1}$) are used to reach high Q. Thus, it is possible at the WNR to analyze liquids diffraction data without introducing questionable models for the inelastic scattering. Note also the competitive count rate of the GPD and the larger Q range obtainable. The water experiment involved taking a linear combination of cross sections obtained on isotope substituted samples ($H_2O$, $D_2O$, and an $H_2O$:$D_2O$ mixture), to extract the HH distinct cross section. Because of the minimal inelasticity effects, this can be compared directly with molecular dynamics simulations of the structure of water as shown in Figure 9. Remarkable overall agreement is obtained between theory and our model independent experiment. The differences correspond to a somewhat smaller coordination number and bond lengths in the experiment compared to the simulations.

The single crystal diffractometer shown in Figure 10 uses a 25 x 25 cm $He^3$ multiwire area detector to collect data in a time resolved Laue technique. Figure 11a shows the intensity as a function of x and y on the detector for the sum of all time channels

in a sapphire sample. Figure 11b shows a single time channel with a single Bragg peak. We have worked closely with ANL in the development of software to derive integrated intensities from the data. Structural refinements on test crystals have produced R factors, thermal parameters, and lattice positions comparable to X-ray and single wavelength reactor experiments. One very encouraging result is that data rates with this instrument at the present WNR are comparable to a four circle diffractometer at BNL. This shows the advantages of the combination of white beams with multidetectors to obtain high data rates. However, backgrounds were much higher than at BNL primarily due to the poor shielding currently available. Upgrade of the instrument will include improved shielding and collimation, a two-axis goniometer, and the use of position sensitive scintillator detectors.

Two instruments are being tested in prototype form. We have developed an eV spectrometer based on the use of nuclear resonances for energy selection (see the article by Brugger, et.al., in these proceedings). The technique is to take the difference between spectra with resonance filters in the beam and removed. Figure 12 shows the scattering from liquid He using the $U^{238}$ resonance at 6.6 eV in a direct geometry. The peak at 3.5 eV energy transfer is from the He while the peak at .69 eV is from the Al container. Tests of resolution in direct, inverted, and sample geometries have been carried out. We are currently examining possible detector configurations. The initial experimental effort is on momentum distributions in hydrogenic systems. We are also developing a

constant Q spectrometer similar to C. Windsor's design primarily for the measurement of high energy elementary excitations in single crystals such as magnons. Considerable attention is being paid to the calibration and alignment of the spectrometer. Resolution calculations suggest that the constant Q machine will have complementary characteristics to triple axis spectrometers at reactors. Preliminary experiments have suggested that competitive data rates will be obtained with the PSR.

We are also addressing several of the technical problems of pulsed sources. This includes chopper phasing (see the article by Bolie, et. al., in these proceedings), beam line collimation and shielding, and scintillator detector development. The approach to collimation and shielding has included empirical tests, the development of detectors to measure neutron energy spectra, and Monte Carlo simulations. The detector effort has concentrated on improving the speed and lowering the $\gamma$ sensitivity of Anger scintillator cameras.

The long range plan for the WNR/PSR is to have a total of eight neutron scattering instruments operational by 1986 when the PSR is expected to come into reliable operation. These include upgraded versions of the filter difference spectrometer (FDS) and single crystal diffractometer (SCD) currently in operation. The present general purpose diffractometer will be replaced by two instruments: one a low resolution (1-2%) machine with small angle capability optimized for liquids, amorphous and special environment diffraction (LIQ); and the other a high resolution ( .15%) powder

diffractometer (HRPD) on a 35 m flight path. We also expect to have a high resolution chopper spectrometer (CS), an eV spectrometer (eVS) and a constant Q machine (CQS) all optimized by research experience on the present WNR. Figure 13 shows a possible layout of condensed matter instruments at the WNR in 1986, where we have added a quasielastic backscattering spectrometer (BSS). The figure also shows the powder diffractometer in low resolution (10m) configuration (LRPD) prior to PSR operation. We show on f.p. 11 that it is possible to place more than one instrument on a beam line if the flight paths are long.

This is a report of work by personnel and collaborators of the neutron scattering group, P-8, at Los Alamos. This includes A. Soper, J. Eckert, J. Goldstone, P. Seeger, P. Vergamini, A. Larson, R. Alkire, R. Brugger (MURR), A. Taylor (Rutherford-Appleton Laboratory) and R. Pynn (ILL).

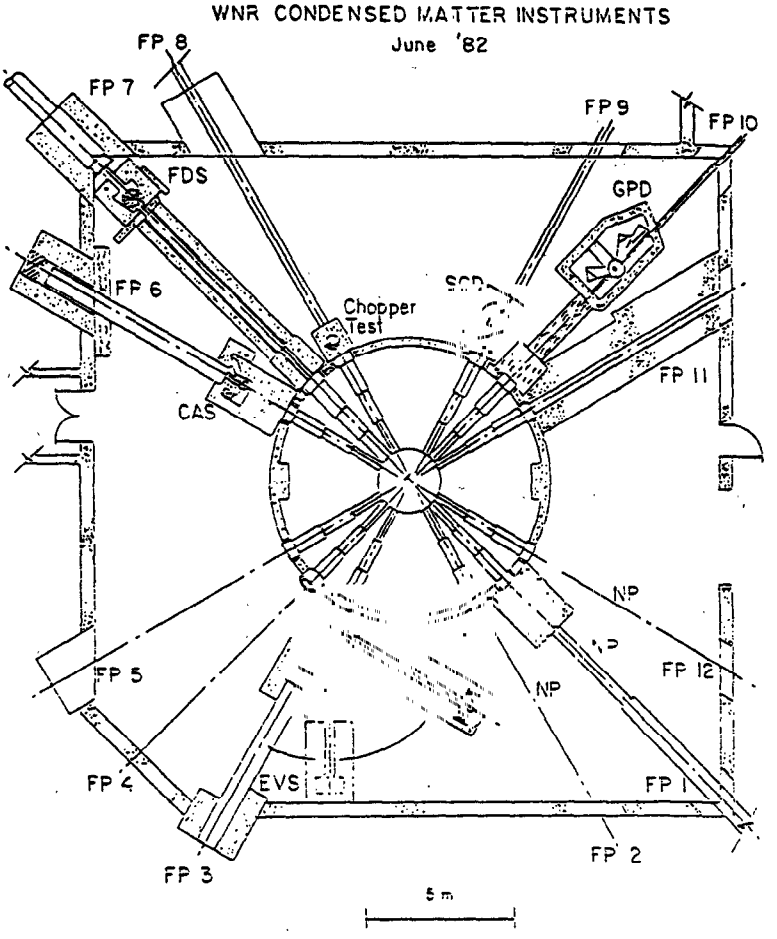


Fig. 1. Current layout of neutron scattering instrumentation at the WNR. NP stands for flight paths assigned to nuclear physics. GPD is the general purpose diffractometer, SCD the single crystal diffractometer, FDS the filter difference spectrometer, CAS the crystal analyzer spectrometer, and EVS the electron volt spectrometer.

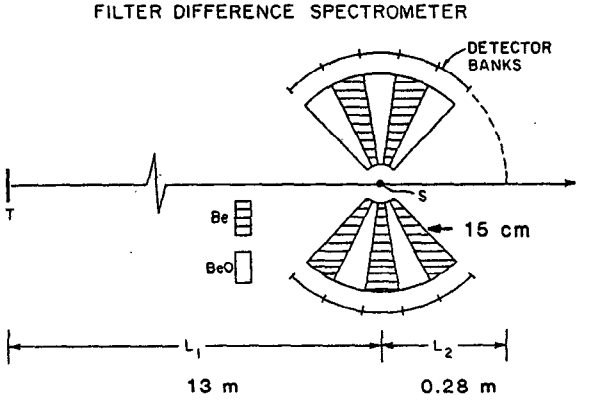


Fig. 2

Schematic layout of the Filter Difference Spectrometer for incoherent inelastic scattering. The filter provides a Bragg cutoff to the final energy bandpass. The difference between Be and BeO filter spectra is taken to improve the resolution of the filter technique. (3b)

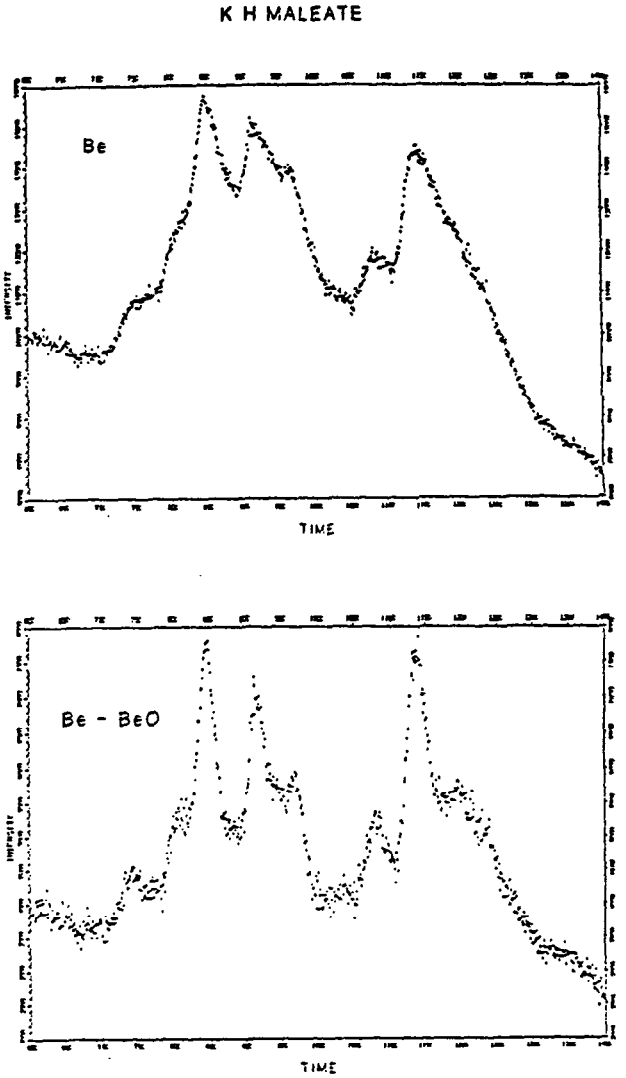


Fig. 3a&b

Comparison of the spectra obtained on KH Maleate using a Be filter (3a) and the Be-BeO filter difference tecnique.

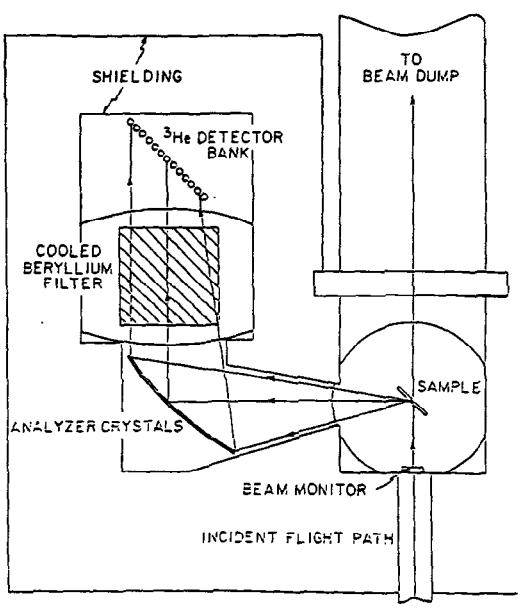


Fig. 4

Schematic layout of the crystal analyzer spectrometer. The analyzer crystals are pyrolytic graphite.

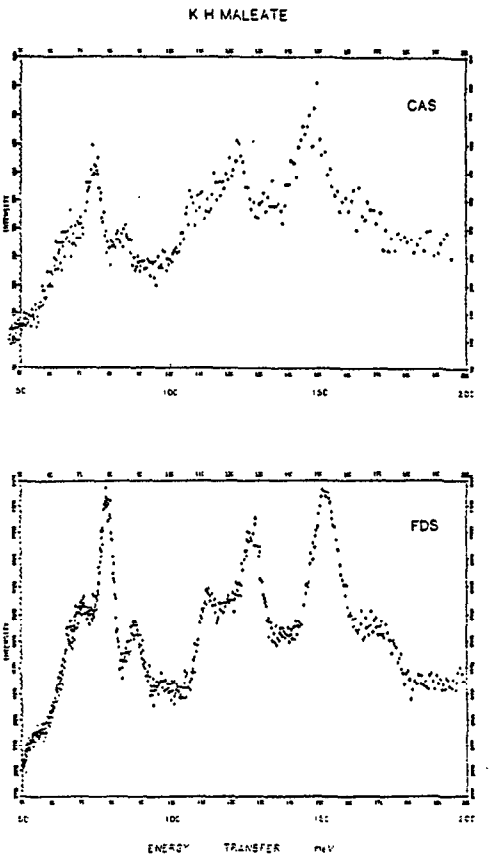


Fig. 5a&b

Comparison of spectra obtained on KH Maleate using the crystal analyzer spectrometer (5a) and the filter difference spectrometer (5b). The FDS has comparable resolution with better count rates. The FDS will be improved another factor of four by cooling the filters and increasing the detector solid angle.

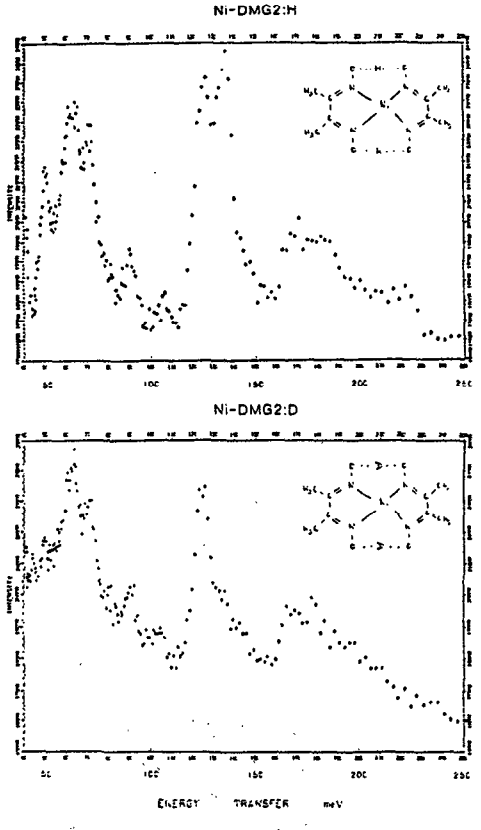


Fig. 5a&b

Incoherent inelastic neutron spectra of nickel dimethylgloxine. H/D substitution is used to identify modes due to the intramolecular hydrogen bond.

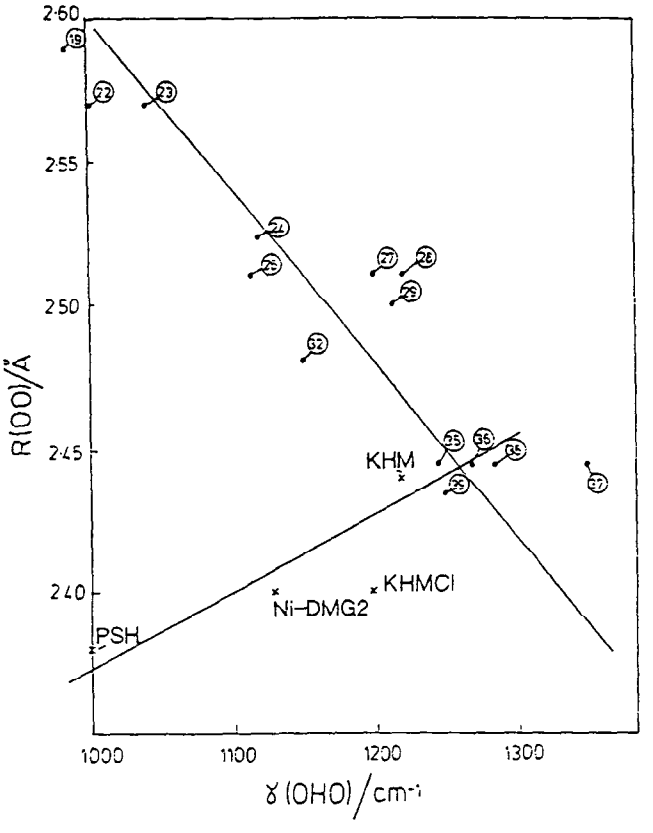


Fig. 7

Variation with bond length of the frequency of the out of plane bending mode in hydrogen bonds. The dots are results for intermolecular hydrogen bonds. The X's are results for intramolecular hydrogen bonds obtained at WNR.

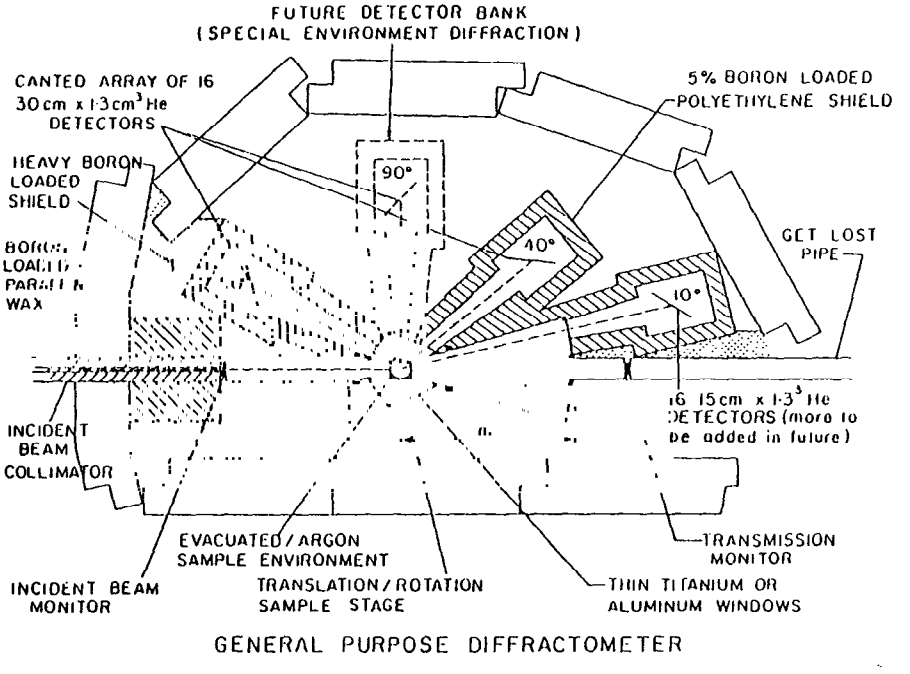


Fig. 8. Layout of the general purpose diffractometer. The sample position is at 10m from the source. The 150° bank provides .45% resolution powder diffraction. The 40° and 10° banks are for liquids diffraction. The evacuated/argon sample environment is under construction.

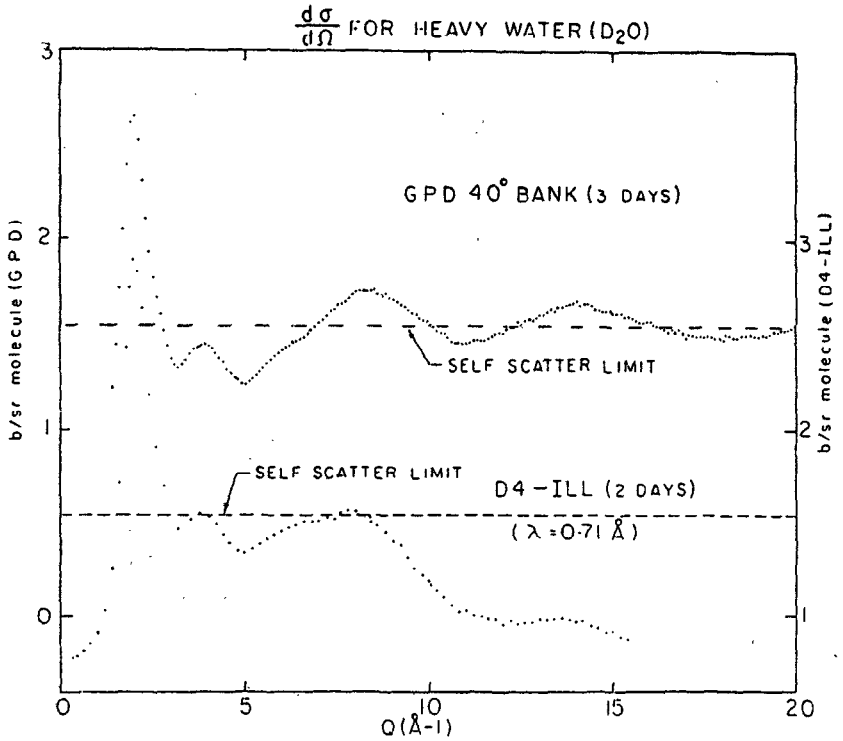


Fig. 9. Comparison of the performance of the GPD at the WNR with the D4 instrument at the ILL. Because inelasticity effects are minimized by reaching high Q with epithermal neutrons at low angles, the GPD results are much closer to the self scattering static limit than the D4 results. Note also the competitive statistics and larger Q range obtainable.

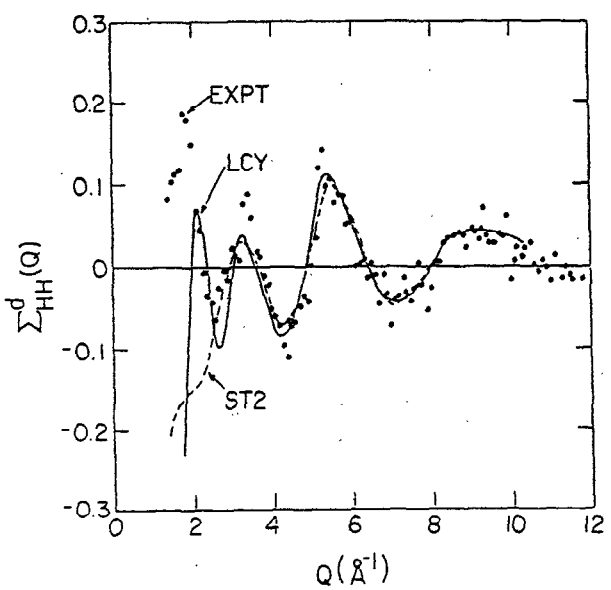


Fig. 10

Distinct hydrogen-hydrogen cross section for liquid water obtained at the WNR. Data are compared to molecular dynamics simulations of water structure using model potentials. LCY stands for Lie, Clementi and Yoshimine. ST2 is the result of Stillinger and Rahman. Data stop at 1.4A$^{-1}$ due to frame overlap on the 40° bank at 120Hz. Data above 12A$^{-1}$ are not shown because of poor statistics. Both problems will be reduced with PSR operation.

# SINGLE CRYSTAL PULSED NEUTRON DIFFRACTOMETER

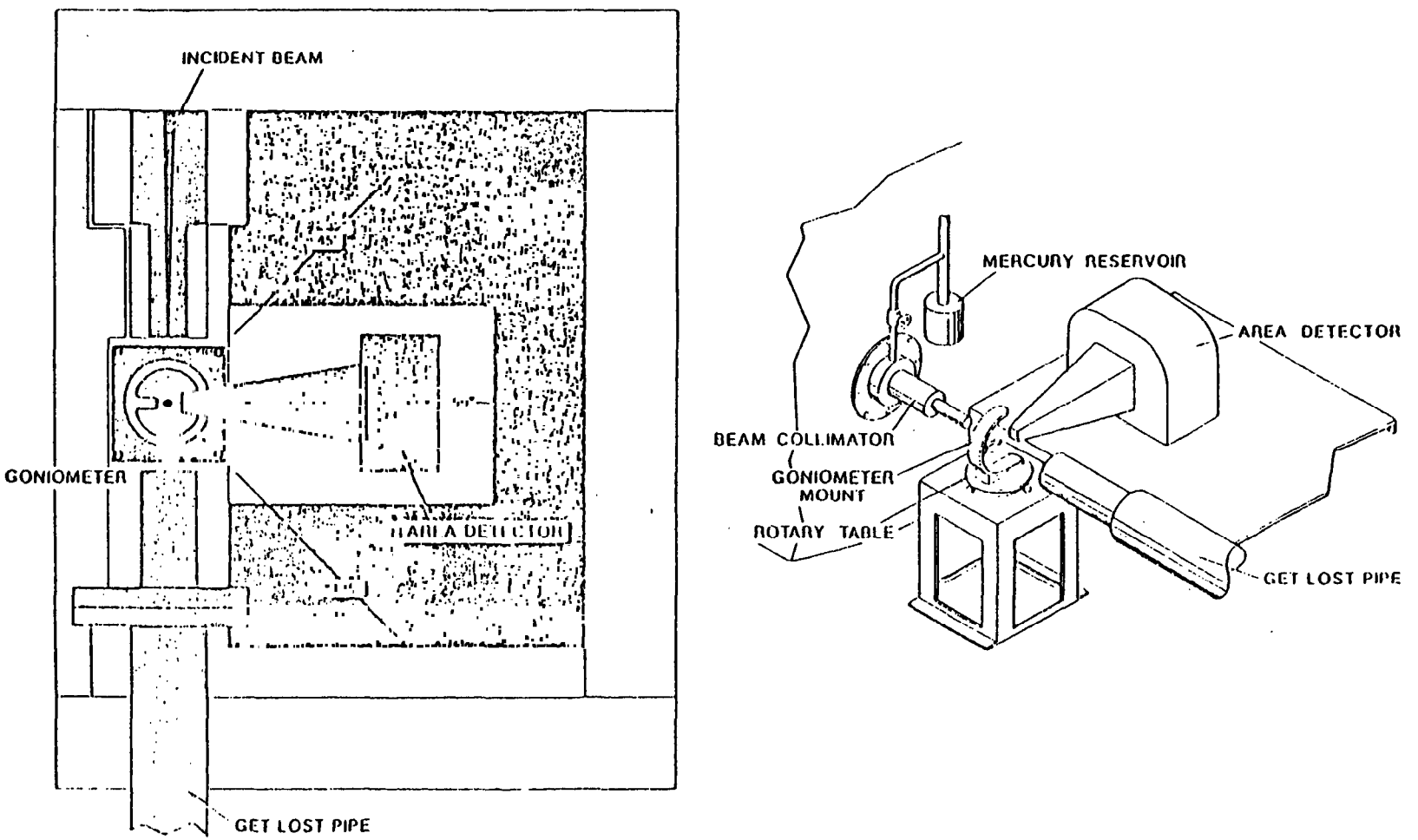


Fig. 11. Layout of the Laue-TOF single crystal diffractometer. The detector is a $He^3$ multiwire counter.

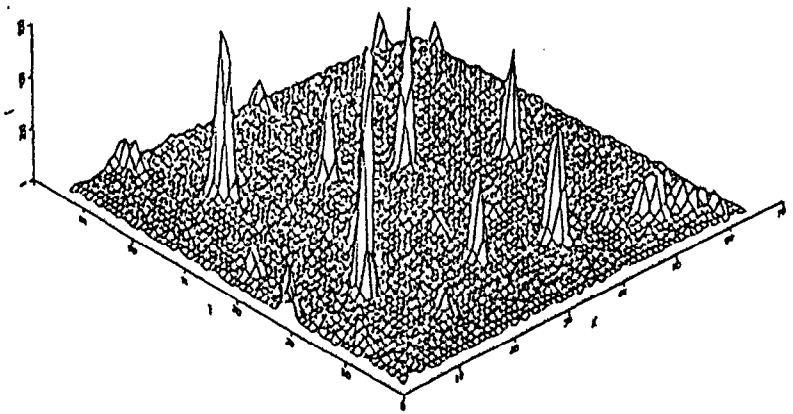

Fig. 12a. Intensity vs position on the area detector for a sapphire crystal with all time channels compressed.

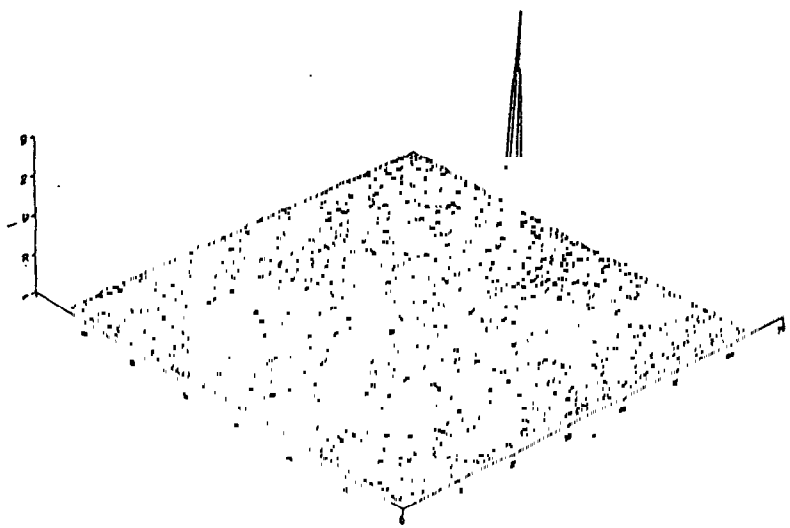

Fig. 12b. Intensity vs position on the area detector for a sapphire crystal and a single time channel.

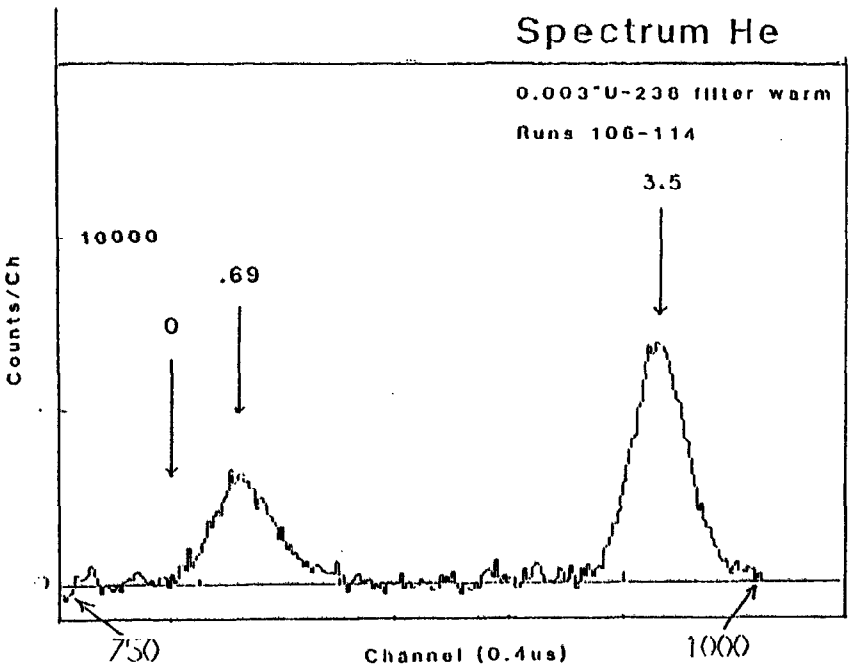


Fig. 13. Inelastic neutron scattering data on liquid He obtained with the electron volt spectrometer using a warm $U^{238}$ filter with a resonance at 6.6 eV. The peak at 3.5 eV transfer is due to the He. The peak at .69 eV transfer is due to the Al container.

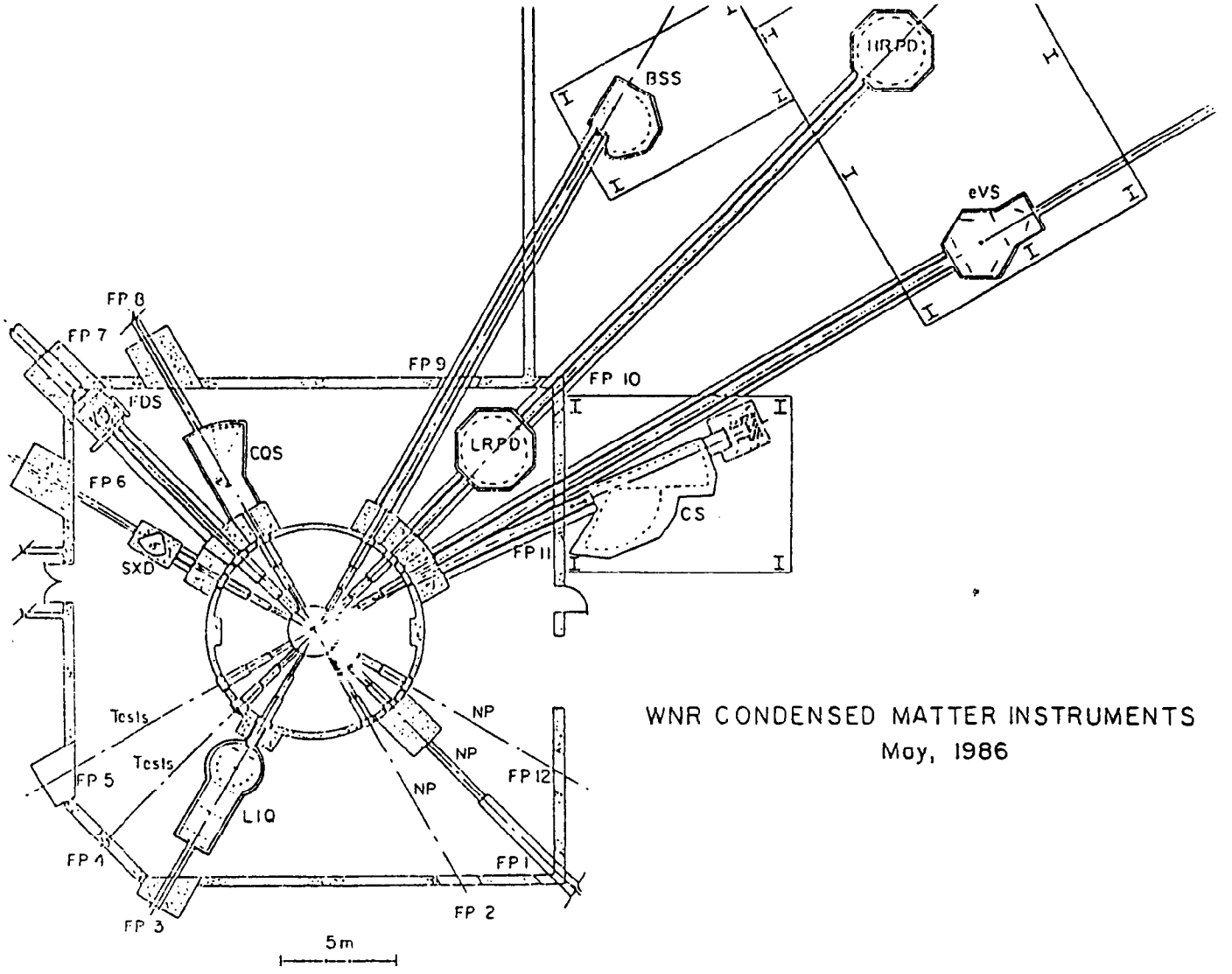


Fig. 14. Possible layout of neutron scattering instruments at the WNR in 1986 after the PSR begins operation. Labels are as in test.

| | | |
|---|---|---|
| J. Meese | Q | What are the milestones for construction of PSR? |
| R. Woods | A | All components should have been delivered in 1984 and construction complete in 1985. |
| J. M. Carpenter | Comment - | You may have been unfair to your results in comparing WNR diffraction data with that from BNL because the BNL background is in 2 dimensions whereas yours is in 3 as a TOF measurement. |
| A. D. Taylor | Comment - | Improving the shielding in a neighboring instrument (the Be filter) reduced the background in the single crystal diffractometer by an order of magnitude. |
| S. K. Satija | Q | What is the background like on the GPD? |
| A. D. Taylor | A | In this case the background arises from air scattering inside the GPD itself. |
| H. Wroe | Q | How long do you think you will take to work PSR up to full intensity? |
| R. Silver | A | About 1 to 2 years. |